

A novel therapeutic strategy for pancreatic neoplasia using a novel RNAi platform targeting PDX-1

Shi-He Liu M.D.¹, Donald D. Rao Ph.D.⁵, John Nemunaitis M. D.^{5,6,7,8}, Neil Senzer M.D.^{5,6,7,8}, David Dawson, M.D., Ph.D.⁹, Marie-Claude Gingras Ph.D.⁴, Zhaohui Wang Ph.D.⁵, Richard Gibbs Ph.D.⁴, Michael Norman M.D.¹, Nancy S. Templeton Ph.D.⁵, Francesco J. DeMayo Ph.D.³, Kelly Stehling B.S.¹, William E. Fisher M. D.^{1,2}, and F. Charles Brunica M.D.^{1,2}.

¹Michael E. DeBaakey Department of Surgery, ²Elkins Pancreas Center, Department of ³Molecular and Cellular Biology, ⁴Human Genome Sequencing Center, Baylor College of Medicine, Houston, Texas; ⁵Gradalis, Inc., ⁶Mary Crowley Cancer Research Centers, Dallas, TX, ⁷Texas Oncology, P.A., Dallas, TX, and ⁸Medical City Dallas Hospital, Dallas, TX; and ⁹Department of Pathology, UCLA School of Medicine, CA

*Address correspondence and reprint requests to F. Charles Brunica, M.D., and Shi-He Liu, M.D.

Michael E. DeBaakey Department of Surgery,
Baylor College of Medicine,
1709 Dryden, Suit 1500, Houston, TX 77030
Phone: 713 798 8070
Fax: 713 798 6609
E-mail: cbrunica@bcm.tmc.edu, sliu1@bcm.edu

Grants:

NIDDK R01-DK46441 and NCI R01 – CA095731, the Vivian L. Smith Foundation, the MD Anderson Foundation, the Elkins Pancreas Center at Baylor College of Medicine, and the generosity of the Bill and Olivia Heintz family

Abstract

Bi-functional shRNA (bi-shRNA), a novel RNA interference (RNAi) effector platform targeting PDX-1 utilizing a systemic DOTAP-Cholesterol delivery vehicle, was studied in three mouse models of progressive pancreatic neoplasia. Species-specific bi-functional PDX-1 shRNA (bi-shRNA^{PDX-1}) lipoplexes inhibited insulin expression and secretion while also substantially inhibiting proliferation of mouse and human cell lines via disruption of cell cycle proteins *in vitro*. Three cycles of either bi-shRNA^{mousePDX-1} or shRNA^{mousePDX-1} lipoplexes administered

intravenously prevented death from hyperinsulinemia and hypoglycemia in a lethal insulinoma mouse model. Three cycles of shRNA^{mousePDX-1} lipoplexes reversed hyperinsulinemia and hypoglycemia in an immune-competent mouse model of pancreatic neoplasia. Moreover, three cycles of the bi-shRNA^{humanPDX-1} lipoplexes resulted in near complete ablation of tumor volume and considerably improved survival in a human PANC-1 implanted SCID-mouse model. Human pancreatic neoplasia specimens also stained strongly for PDX-1 expression. Together, these data support the clinical development of a novel therapeutic strategy using systemic bi-shRNA^{PDX-1} lipoplexes against pancreatic neoplasia.

Pancreatic and duodenal homeobox-1 (PDX-1) is a transcription factor that plays a critical role in regulating embryologic pancreas development as well as in insulin expression and islet maintenance in the adult pancreas¹⁻⁴. PDX-1 has recently been shown to play a significant role in islet cell neoplasia and pancreatic cancer⁵⁻¹¹. PDX-1 knockout is lethal in mice and mutation of PDX-1 leads to mature onset of diabetes of the young (MODY subtype IV) in mice and human patients^{12,13}. Persistent overexpression of PDX-1 leads to acinar to ductal cell metaplasia in mice¹⁴. Overexpression of PDX-1 in cell lines results in transformation of non-insulin-producing cells into insulin-producing cells upon GLP-1 stimulus¹⁵⁻²⁰. Although PDX-1 is well known as an essential regulator of many pancreatic endocrine genes (e.g., insulin¹⁻⁴, glucokinase²¹, islet amyloid polypeptide²²⁻²⁴, glucose transporter type 2 [GLUT2]^{25,26}, pancreatic polypeptide²⁷ and somatostatin^{6,28}), which have critical roles in maintaining glucose homeostasis (e.g., insulin and glucokinase), the precise role of PDX-1 in pancreatic neoplasia remains unknown.

Our recent studies demonstrate that PDX-1 is a potential oncogene and a therapeutic target for pancreatic neoplasia^{11,29}. It is markedly overexpressed in pancreatic cancer^{8,10,11,30} and regulates proliferation and invasion of human pancreatic cancer cells *in vitro* and *in vivo* in mice¹¹. PDX-1 over-expressing cells have increased tumor formation when implanted in mice²⁹. We have previously demonstrated that shRNA^{humanPDX-1} lipoplexes effectively ablate human pancreatic cancer tumor formation in SCID mice, resulting in prolonged survival¹¹.

In this study, the activity of a novel RNAi effector platform targeting PDX-1 was studied *in vitro* and *in vivo* in human and mouse cell lines as well as in mouse models of progressive pancreatic neoplasia.

Results

PDX-1 is overexpressed in human and mouse specimens of progressive pancreatic neoplasia

PDX-1 was overexpressed in 36 human pancreatic neoplasia specimens including 26 pancreatic neuroendocrine tumors (Fig. 1a-l) and 10 nesidioblastosis specimens (Fig. 1m-o), in mouse insulinoma (β TC-6) cells (Fig. 1p) and in both islets and acinar cells of the pancreas of SSTR1/5^{-/-} mice (Fig. 1r, s and t, respectively). These data demonstrate PDX-1 is significantly overexpressed in both human and mouse specimens of progressive pancreatic neoplasia and are consistent with PDX-1 overexpression as seen in our former study of 80 human pancreatic cancer specimens⁸.

Bi-shRNA^{mousePDX-1} knockdown of PDX-1 expression in β TC-6 cells *in vitro* inhibits insulin expression and secretion via inhibition of the insulin promoter.

Bi-shRNA^{mousePDX-1} resulted in significantly greater knockdown of PDX-1 expression in β TC-6 cells at doses of 6 μ g and 12 μ g per 10-cm dish than shRNA^{mousePDX-1} and empty vector controls in both western blot (Fig. 2a; p<0.05) and immunohistochemistry (IHC) analyses (Fig. 2b top panel). Bi-shRNA^{mousePDX-1} resulted in significantly greater inhibition of insulin expression (32 \pm 3.2% vs

62±6.3% vs 93±9.9%) and PDX-1 expression (28±2.7% vs 51±4.5% vs 97±7.3%) than that seen with shRNA^{mousePDX-1} and empty vector control cells, respectively (Fig. 2c, p<0.05; and Fig. 2b). Transfection with bi-shRNA^{mousePDX-1} resulted in significantly greater inhibition of glucose-stimulated insulin secretion from β TC-6 cells *in vitro* compared to that seen with shRNA^{mousePDX-1} and empty vector controls at glucose concentrations of 5 and 11 mM (p<0.05), respectively (Fig. 2d). These findings indicate that bi-shRNA^{mousePDX-1} inhibits insulin expression and secretion via PDX-1 knockdown to a greater degree than conventional shRNA^{mousePDX-1} in mouse insulinoma cells.

To further delineate the mechanism by which knockdown of PDX-1 inhibits insulin expression and secretion through reduced activation of rat insulin promoter-1(RIP), reporter constructs (RIP-mCherry) with or without shRNA^{mousePDX-1} were transfected into β TC-6 cells. RIP-mCherry-H1-shRNA^{mousePDX-1} resulted in significant reduction in mCherry expression as compared to that of RIP-mCherry without shRNA^{mousePDX-1} (10±1.6% vs 35±8.1% and 12±2.1% vs 66±13.2% at 24h and 48h, respectively, p<0.05; Fig. 2e). Transfection of RIP-mCherry-CMV-eGFP-H1 revealed that 90% of cells were successfully transfected, as evidenced by eGFP expression. Additionally, 69% of eGFP-expressing cells expressed mCherry, and in RIP-mCherry-CMV-eGFP-H1-shRNA^{mousePDX-1} transfected cells, 88% of cells expressed eGFP; however, only 12% of cells expressed mCherry (p<0.05; Fig. 2f). Decreased PDX-1 expression was confirmed using western blot. These data suggest that activation of the insulin promoter is significantly inhibited by shRNA^{mousePDX-1} via knockdown of PDX-1 expression.

Species-specific Bi-shRNA^{PDX-1} knockdown of PDX-1 expression inhibits proliferation in mouse insulinoma and human PANC-1 cells.

Significant suppression of cell proliferation was observed in β TC-6 cells transfected with bi-shRNA^{mousePDX-1}. Reductions in cell growth were observed at 52%, 38%, and 31% in empty vector controls at 24, 48, and 72h post-transfection, respectively, using MTS assay (Fig. 3a) and at 42%, 35%, and 42%

at 12, 24, and 48h post-transfection, respectively, using BrdU incorporation assay (Fig. 3b) ($p < 0.05$ at all time points). Bi-shRNA^{mousePDX-1} resulted in greater inhibition of cell proliferation than shRNA^{mousePDX-1} at low doses (6 μ g/10-cm dish) after 48h of transfection (Fig. 3d). Cell cycle protein analysis demonstrated down-regulation of positive regulators cyclin E, Cdk2, and Cdk4, and up-regulation of negative regulators p53 and p27, in bi-shRNA^{mousePDX-1}-treated cells compared to that of empty vector ($p < 0.05$, respectively; Fig. 3e). Similarly, bi-shRNA^{humanPDX-1} transfection of PANC-1 cells resulted in a reduction of cell proliferation by 58%, 40% and 38% of empty vector controls at 24, 48 and 72h post-transfection, respectively, with greater inhibition of cell growth than shRNA^{humanPDX-1} at low doses (6 μ g or 12 μ g/10-cm dish)(Fig. 3f, 3g). These data demonstrate that species-specific PDX-1 knockdown inhibits mouse insulinoma cell and human pancreatic cancer cell proliferation via alterations in cell cycle proteins.

Systemic bi-shRNA^{mousePDX-1} lipoplexes prevent death from hyperinsulinemia and hypoglycemia in an insulinoma SCID mouse model.

Three cycles of systemic bi-shRNA^{mousePDX-1} lipoplexes (25 μ g /mouse biweekly) or shRNA^{mousePDX-1} lipoplexes (35 μ g /mouse biweekly) prevented death from hyperinsulinemia and hypoglycemia (Fig. 4a and b, and c and d, respectively) in a lethal insulinoma SCID mouse model. Transient hyperglycemia and hypoinsulinemia were observed, but levels returned to baseline on day 150 after the initial treatment in both treatment groups. Empty vector lipoplexes had no effect on lethal hyperinsulinemia and hypoglycemia, as shown in Fig. 4a and b. Overall survival in both treatment groups was significantly longer than that of controls (106 \pm 7.8d vs 53 \pm 1.4d and 146 \pm 9.5d vs 53 \pm 1.4d, respectively, $p < 0.05$ vs controls, Fig. 4f and g, sFig. 1). The difference in survival between the two treatment groups was due to intentional sacrificing of that group of mice at an earlier time point, but there is no significance ($p > 0.05$)(sFig. 1f). These data demonstrate that PDX-1 knockdown using systemic bi-shRNA^{mousePDX-1}

lipoplexes effectively prevent hypoglycemic death in an insulinoma SCID mouse model.

Remarkably, systemic bi-shRNA^{mousePDX-1} and shRNA^{mousePDX-1} lipoplexes result in temporal hyperglycemia, representing a predictable off-target effect in mouse islets. After treatment with bi-shRNA^{mousePDX-1}, *in situ* islet PDX-1 expression was reduced in a treatment-dependent manner, from 88±10.1% on day 0 to 71±8.6%, 49±9.7% and 23±6.6% on days 7, 21, 35 after the initial treatment, respectively, and returned to 83±12.4% at the time of sacrifice, as shown in the Fig. 4e, top panel. Interestingly, insulin expression also was significantly decreased from 92±8.3% on day 0 to 61±9.8%, 32±5.3%, 12±1.9% on days 7, 21, 35 after the initial treatment, respectively, and returned to 89±15.3% at the time of sacrifice, as shown in Fig. 4e, 2nd panel. Expression levels of PP also decreased significantly at the same time points after treatment (Fig. 4e, 3rd panel). Markers of islet cell proliferation, cell cycle proteins and apoptosis were also studied pre- and post-treatment. Islet PCNA expression significantly decreased from 16±1.4% to 10±0.8%, 7±0.6%, 5±0.2% and 14±2.0% on days 0, 7, 21, 35 and upon sacrificing, respectively (Fig. 4e, 4th panel). IHC analysis of pancreatic sections demonstrated increasing p27 expression and decreasing expression of protein levels in cyclin E and Cdk4 on days 0, 7, 21, 35, and upon sacrificing following three cycles of treatment (Fig. 4e 5, 6 and 7th panel to top, respectively). This is consistent with the findings from western blot analyses of whole pancreata (sFig. 2). Bi-shRNA^{mousePDX-1} resulted in a significant increase in apoptosis of mouse islets from 1 ±0.2% on day 0, to 14 ±2.4%, 24 ±3.6%, 42±5.5%, 10±1.1% on days 7, 21, 35 and upon sacrificing, respectively (Fig 4e bottom panel). Empty vector control therapy had no effect on islet PDX-1, insulin, PP expression, cell cycle proteins and apoptosis. These data are consistent with findings seen following PDX-1 knockdown in mouse insulinoma cells *in vitro*. They also suggest that systemic bi-shRNA^{PDX-1} lipoplexes result in temporal, mild hyperglycemia emanating from suppression of PDX-1 within the islets of Langerhans with subsequent suppression of insulin and PP expression, correlating with alterations

in islet cell cycle proteins and an increase in islet apoptosis. Expression of all islet markers returned to baseline values upon sacrificing, suggesting a regenerative capacity of murine islets. Similar patterns of expression of PDX-1, insulin, PP, and cell cycle proteins and apoptosis in islet cells also was observed after three cycles of shRNA^{mousePDX-1} lipoplexes (sFig. 3). These data demonstrate that systemic bi-shRNA^{mousePDX-1} lipoplexes effectively prevent hypoglycemic death in an insulinoma SCID mouse model and result in *in situ* knockdown of PDX-1 with the islets leading to suppression of insulin expression and subsequent hyperglycemia. Remarkably, any off-target islet effects were mild and temporal, suggesting a regenerative capacity of the murine endocrine pancreas.

Systemic shRNA^{mousePDX-1} lipoplexes reverse hyperinsulinemia and hypoglycemia and alter glucose tolerance in somatostatin receptor subtypes 1 and 5 (SSTR1/5^{-/-}) knockout mice

Three cycles of shRNA^{mousePDX-1} lipoplexes (35µg /mouse) significantly reversed both hyperinsulinemia and hypoglycemia in SSTR1/5^{-/-} mice (3±0.2 µg/l and 83±19.5mg/dl on day 0 and 0.5±0.1 µg/l and 205±25.9 mg/dl on day 35 after the initial treatment, respectively, as seen in Fig. 5a and b). Systemic glucose and insulin levels returned to baseline on day 150 after the initial treatment, although systemic insulin levels were significantly lower in the treatment group than in controls (3.1±0.2 µg/l vs 2±0.6 µg/l, p<0.05). Empty vector lipoplexes were without effect on hyperinsulinemia and hypoglycemia (Fig. 5a and b). Islet PDX-1 expression was reduced in a treatment-dependent manner, from 93±13.5% on day 0 to 12±2.6% on day 35 post-treatment; returning to 88±15.2% on day 150 post-treatment (Fig. 4c, top panel). Islet PCNA expression decreased significantly from 33 ±2.8 to 6±0.6% and to 29 ±4.3% on days 0, 35 and 150d post-treatment, respectively (Fig. 5c middle panel), which correlated to down-regulation of cyclin E, cyclin D, Cdk4 and Cdk2. No effect was seen with empty

vector controls ($p < 0.05$; Fig. 5d). Increased islet cell apoptosis also was observed ($1 \pm 0.1\%$, $19 \pm 3.2\%$, $32 \pm 5.7\%$, $58 \pm 8.9\%$ and $9 \pm 1.4\%$ on days 0, 7, 14, 35 and 150 post-treatment, respectively, Fig. 5c bottom panel). Intraperitoneal glucose tolerance tests (IPGTT) were performed on *SSTR1/5^{-/-}* mice at day 7 and 150 after the initial treatment. Fasting glucose levels in the treated group were significantly higher than that of controls (117 ± 6.8 mg/dl vs 84 ± 5.9 mg/dl, $p < 0.05$), whereas basal insulin levels in the treatment group were lower than those of controls (1 ± 0.1 μ g/l vs 2 ± 0.2 μ g/l, $p < 0.05$; Fig 5d). Following intraperitoneal glucose injection, systemic glucose levels were significantly higher than those of controls at 60 and 240 min post-injection (234 ± 20.2 mg/dl vs 189 ± 21.0 mg/dl and 175 ± 11.3 mg/dl vs 137 ± 16.8 mg/dl, respectively $p < 0.05$). Serum insulin levels were significantly lower than those of controls at 15 min post-injection (2 ± 0.1 μ g/l vs 3 ± 0.2 μ g/l) (Fig. 5e). On post-treatment day 150, no significant difference in basal glucose levels was seen between treatment and control groups; however, basal insulin levels in the treatment group were significantly lower than in those of controls (1 ± 0.3 μ g/l vs 2 ± 0.3 μ g/l, $p < 0.05$). Only the 15-min time point demonstrated a significant difference in systemic glucose levels between the groups (364 ± 60.1 vs 267.0 ± 40.4 , $p < 0.05$). Systemic insulin levels; however, were significantly lower at the 30- and 120-min time points in the treatment group as compared to controls, (2.2 ± 0.3 μ g/l vs 3.3 ± 0.2 μ g/l and 2.5 ± 0.1 μ g/l vs 3.8 ± 0.3 μ g/l at 30 and 120 min post-injection, respectively; $p < 0.05$) (Fig. 5g).

These data demonstrate that three cycles of systemic shRNA^{mousePDX-1} lipoplexes are well tolerated and effective in reversing hyperinsulinemia and hypoglycemia in an immune-competent mouse model of pancreatic neoplasia. Significant alterations in glucose tolerance seven days after the initial treatment corresponded with suppressed islet PDX-1 and insulin expression. Mild alterations in the response to IPGTT seen at 150 days post-treatment correspond

with normalization of islet PDX-1 and insulin expression and suggest a regenerative capacity of immune-competent murine islets.

Systemic shRNA^{humanPDX-1} lipoplexes reduce tumor volume and prolong survival in a human pancreatic cancer xenograft SCID mouse model

PANC-1 cells are human pancreatic cancer cells (PANC-1) that markedly overexpress PDX-1, and when placed intraperitoneally, grow large tumors in SCID mice. Three cycles of bi-shRNA^{humanPDX-1} lipoplexes (35µg/mouse) significantly reduced PANC-1 tumor volume with only a few mice having residual tumors averaging 50.5 mm³ compared to 100% of control mice with tumors averaging 1199 mm³ at 90 days post-treatment, respectively (p<0.05; Fig 6a). Survival was significantly longer than controls (115±9.5d vs 85±1.4d, respectively; (p=0.001; Fig. 6b) with no significant difference in survival between control vector-treated mice and untreated mice (85±9d vs 76±8d, p=0.981). In those mice with residual tumors, tumor PDX-1 expression significantly reduced from 95±11.1% to 12±1.3% on days 0 and 90 post-treatment, respectively (Fig. 6c top panel). IHC analysis of residual tumors revealed cell proliferation markers, PCNA and Cyclin E, had decreased expression from 84±9.6% and 66±10.2% to 15±0.8% and to 9±2.3%, respectively (Fig. 6C 2nd and 3rd panels), and an increase in P53 expression (Fig 6c, 4th panel). Marked apoptosis was seen in residual tumors (Fig. 6c, bottom panel). Remarkably, three cycles of bi-shRNA^{humanPDX-1} lipoplexes had no effect on systemic glucose and insulin levels, underscoring the importance of the species-specific design of PDX-1 RNAi (sFig. 4).

These data demonstrate that multiple cycles of systemic shRNA^{humanPDX-1} lipoplexes were well tolerated and effectively reduced human pancreatic cancer tumor volume and prolonged survival in SCID mice, suggesting a clinical potential of this novel therapeutic strategy for the most aggressive form of pancreatic neoplasia.

Discussion

This study demonstrates that multiple cycles of a novel RNAi effector platform targeting PDX-1 utilizing a systemic DOTAP-Cholesterol delivery vehicle are well-tolerated and effective in three mouse models of progressive pancreatic neoplasia. These findings are consistent with our previous studies that PDX-1 is a therapeutic target for pancreatic neoplasia^{11,29}. Data from the current study has demonstrated marked overexpression of PDX-1 in human specimens of pancreatic neoplasia. This, combined with our prior findings of PDX-1 expression in the most aggressive form of pancreatic neoplasia, pancreatic cancer⁸, supports the clinical application of this novel RNAi platform³¹.

Our novel RNAi platform was used to knockdown PDX-1 expression *in vitro* and *in vivo*. Although synthetic small interfering RNAs (siRNAs) are easier to deliver in preclinical investigations and have recently entered clinical studies, DNA cassettes that express small hairpin RNA (shRNA), microRNA (miRNA), or strands of siRNAs have the advantage of prolonged effect^{32,33}. Transcribed shRNA from an expression vector intrinsically differs from siRNA with respect to intracellular trafficking and nucleotide preference and the bi-shRNA construct can further enhance gene knockdown³¹. Our novel bifunctional RNAi vector represses translation of the target mRNA via both cleavage-independent and cleavage-dependent RISC loading pathways, resulting in differential Argonaute incorporation and separate, but coordinated, target inactivation mechanisms³¹.

In order to achieve multiple intravenous doses of the RNAi therapy, the liposomal delivery system used in this study was developed using 1,2-dioleoyl-3-trimethylammonio propane (DOTAP) and cholesterol bilamellar invaginated vesicle (BIV)³⁴. BIV envelope the RNAi expression vector creating a lipoplex, which achieve low morbidity, effective, and multiple sequential intravenous dose scheduling of the RNAi therapeutic³⁴. The composition and structure of these lipoplexes result

in an optimized ~5½ hour plasma half-life by minimizing interaction with plasma proteins and accumulation in non-target tissues; their fusogenic property avoids endocytosis, which otherwise can lead to nucleic acid degradation³⁵. The safety of this lipoplex system to be administered intravenously in multiple cycles already has been demonstrated in other in vivo models to other targets^{36,37} and clinical trials^{38,39}.

In a xenograft mouse model of human pancreatic cancer, the most aggressive form of pancreatic neoplasia, our strategy of PDX-1 knockdown effectively reduced human pancreatic cancer tumor formation in SCID mice and prolonged survival¹¹. It was remarkable that in the few mice with residual pancreatic cancer tumors, studies of those tumors revealed marked suppression of PDX-1 and marked enhancement of both P53 and apoptosis 90 days after therapy. This suggests that PDX-1 knockdown activated the apoptotic pathway via P53 within PANC-1 cells, similar to *in vitro* data seen in our previous study as well as that seen in insulinoma cell lines in this study. These findings support the concept that PDX-1 has oncogenic properties and is a potential therapeutic target for pancreatic cancer. We previously reported that 80 human pancreas tissue specimens, including liver metastases, had marked overexpression of PDX-1^{8,11,29}. Together, these findings support the development of a phase I clinical trial using this novel RNAi platform targeting PDX-1 for treating this devastating form of pancreatic neoplasia. Interestingly, there was no adverse effect on islet PDX-1 or insulin expression, as well as insulin and glucose levels in mice, demonstrating the importance of species-specificity of the PDX-1 shRNA design.

Insulinoma is an intermediate form of pancreatic neoplasia in which tumor formation occurs with a ratio of approximately 90% benign and 10% malignant. The effect of PDX-1 knockdown on mouse insulinoma cells revealed 1) deactivation of an exogenous rat insulin promoter fragment; 2) decreased activation of endogenous insulin promoter resulting in inhibition of expression and secretion of insulin 3) inhibition of proliferation via alterations on cell cycle

proteins, 4) prevention of lethal hypoglycemia in an insulinoma SCID mouse model and 5) temporal suppression of islet PDX-1 and insulin expression associated with mild hyperglycemia. It is to be noted that due to the rapid occurrence of malignant hypoglycemic death, there is insufficient time for implanted β TC-6 insulinoma cells to develop into measurable lesions before insulinoma-induced hypoglycemic death; therefore, there is no tumor volume to be measured in this model. However, the systemic effect of the remarkable suppression of *in situ* islet PDX-1 with associated suppression of insulin and PP, both known to regulate glucose homeostasis²²⁻²⁴ and increased islet apoptosis, suggests the development of temporal mild hyperglycemia post-therapy is due to the effect of bi-shRNA^{mousePDX-1} lipoplexes on the endocrine pancreas.

Furthermore, this demonstrates that systemic delivery of the effector platform reaches its PDX-1 target. The survival advantage following multiple systemic cycles of bi-shRNA^{mousePDX-1} lipoplexes suggests that mild, transient hyperglycemia is an acceptable off-target toxicity in exchange for anti-neoplasia activity^{1-4, 27}

Combined with the finding that 36 human pancreatic neoplasia specimens had marked overexpression of PDX-1, these data suggest that our novel RNAi effector platform has clinical potential for treating pancreatic neuroendocrine tumors, which includes both malignant and benign forms of pancreatic neoplasia, as well as nesidioblastosis⁴⁰. Furthermore, since there are no current effective treatments for the devastating hormonal symptoms associated with pancreatic neuroendocrine tumors⁴⁰, this study suggests another potential clinical application for the novel RNAi effector platform targeting PDX-1 is the control of symptoms associated with excessive hormonal secretion associated with pancreatic neoplasia.

Our laboratory has a long history studying the role of somatostatin receptors (SSTRs) in islet physiology⁴¹⁻⁴⁴. We first demonstrated that mouseSSTR5 was the SSTR subtype responsible for inhibiting glucose-stimulated insulin secretion

from mouse islets and then cloned the mouse *SSTR5* gene. *SSTR5*^{-/-}, beta cell-specific *SSTR5*^{-/-} and *SSTR1/5*^{-/-} mouse models were then generated in our laboratory⁴⁵. Phenotyping of these mice revealed that *SSTR1/5*^{-/-} mice develop basal hypoglycemia, circulating hyperinsulinemia, and are associated with islet neoplasia and marked overexpression of islet and acinar PDX-1⁴¹.

In these immune-competent mice, multiple cycles of iv shRNA^{mousePDX-1} lipoplexes were well tolerated and reversed hyperinsulinemia and hypoglycemia. Similar to the results seen in the insulinoma SCID mouse model, *SSTR1/5*^{-/-} mice developed temporal hyperglycemia associated with suppression of islet PDX-1, insulin and PP expression, disruption of cell cycle proteins, and increased islet apoptosis. Glucose tolerance tests revealed elevated basal glucose levels, lower insulin levels and an abnormal response to IPGTT seven days after the first treatment. These results suggest that the hyperglycemia is due to suppression of insulin secretion, which would be consistent with suppressed islet PDX-1 and insulin expression and enhanced islet apoptosis. Remarkably, these mice have almost complete restoration of their response to glucose intolerance associated with the normalization of islet PDX-1, insulin, PP and PCNA expression, as well as absence of islet apoptosis, suggesting the regenerative capacity of the murine endocrine pancreas in this immune-competent mouse model of pancreatic neoplasia⁴⁶⁻⁴⁸.

In summary, PDX-1, which exhibits both oncogenic and hormonal-regulatory properties, is a therapeutic target in three mouse models of progressive pancreatic neoplasia. Multiple cycles of systemic PDX-1 RNAi lipoplexes were well tolerated in both immune-deficient and immune-competent mice. Bi-shRNA^{humanPDX-1} lipoplexes nearly completely ablated human pancreatic cancer tumor volume in SCID mice and prolonged survival. Bi-shRNA^{mousePDX-1} lipoplexes prevented death from hypoglycemia and hyperinsulinemia in an insulinoma mouse model and reversed hyperinsulinemia and hypoglycemia in an immune-competent mouse model of pancreatic neoplasia. In these models,

murine specific shRNA^{mousePDX-1} was associated with mild temporal hyperglycemia due to suppression of *in situ* islet PDX-1 expression and related islet hormones, as well as enhanced islet apoptosis, demonstrating effective systemic delivery of the platform to the PDX-1 target and suggesting regenerative capacity for the murine endocrine pancreas following treatment. This study demonstrates the potential of a novel RNAi effector platform targeting PDX-1 using liposome delivery as a therapeutic strategy for pancreatic neoplasia.

Methods

Cell lines, vectors, and antibodies. Mouse β TC-6 and PANC-1 cell lines were obtained from the American Type Culture Collection (ATCC, Bethesda, MD). Mouse PDX-1 shRNA (shRNA^{mousePDX-1}) was designed as previously described¹¹. Bi-functional mouse (bi-shRNA^{mousePDX-1}) and human PDX-1 (bi-shRNA^{humanPDX-1}) was obtained from Gradalis Inc. pRIP-mCherry_CMV-eGFP and pRIP-mCherry_CMVeGFP_H1-shRNA^{mousePDX-1} were subcloned based on the parent vector RIP-mCherry-NLS-mCherry which was kindly provided by Dr. Michael Mancini from Baylor College of Medicine. Goat anti-rabbit anti-serum and sheep anti-mouse anti-serum conjugated with horseradish peroxidase were purchased from Amersham (Amersham Life Science Inc., Arlington Heights, IL). Rabbit anti-goat IgG was obtained from ZYMED (Zymed Laboratories, Inc. South San Francisco, CA, USA).

Transfection and reporter assay. β TC-6 or PANC-1 cells were plated into 10-cm cell culture plates at 1×10^6 cells per dish or 24-well plates at 1×10^5 cells/well and incubated at 37°C for 24 h. Transfection assays were performed using Lipofectamine 2000 (Invitrogen, Carlsbad, CA, USA) according to manufacture's instruction. Fluorescence signals were observed and counted using fluorescence microscopy as previous described¹¹ to determine the reporter activities.

Cell proliferation assay *in vitro*. Cell proliferation was determined by MTS assay (Promega, Madison, WI) and BrdU incorporate assay (colorimetric) (Roche

Diagnostica GmbH, Mannheim, Germany) at 12, 24, 48 and 72h post transfection. Absorbance was read in a Multiskan EX plate reader (Thermo Electronic Corp., Franklin, MA) at 492 nm for MTS and 500nm for BrdU assay and levels of proliferation were calculated as described previously

Western blot analyses. Forty-eight hours after transfection, as described previously¹¹, β TC-6 cells were collected and lysed in RIPA buffer. 20 μ g of cell lysates were applied to SDS-PAGE gel for electrophoresis. The protein was then transferred to membranes to be probed with various antibodies against PDX-1, cyclinD1, cyclin E, Cdk2, Cdk4, and p27. Immunocomplexes were visualized by enhanced chemiluminescence (ECL) detection using horseradish peroxidase conjugated secondary antibodies.

Animals and shRNA Delivery. SCID mice were housed in a BL-4 facility and cared in compliance with the guidelines in *The Care and Use of Laboratory Animals* prepared by the Institute of Laboratory Animal Resources, the Commission on Life Science, the National Research Council and the Animal Research Committee of Baylor College of Medicine. DNA Doses were determined by meeting the criteria of less than 10% mouse death after injection of liposomal shRNA complex in regular SCID mice. Age 8- to 10-week-old male mice were inoculated with 1×10^6 β TC-6 or PANC-1 cells per mouse via intraperitoneal (ip) injection. Two weeks later, either β TC-6 or PANC-1 mice were randomly grouped (30 mice per group) and the first cycle of shRNA^{mousePDX-1} or bi-shRNA^{mousePDX-1} or bi-shRNA^{humanPDX-1}, respectively, were given via tail vein injection. The cycles were repeated at days 14 and 28 for a total of three injections. The same protocol was applied to SSTR1/5^{-/-} mice using 3 cycles of 35 μ g of shRNA^{mousePDX-1}.shRNA^{mousePDX-1}. The PDX-1 RNAi complexes were prepared as previously described¹¹.

Insulin and glucose measurements. On days 7, 21, 35, and 150 following each gene delivery, 50 μ l whole blood samples were collected and spun to separate the serum. Glucose levels were measured using a Beckman-Coulter Glucose Analyzer 2 (Coulter-Beckman, Fullerton, CA), and presented as mean \pm S.E.M.

in mg/dl. Insulin levels were determined using a mouse insulin ELISA kit from Mercodia (Linco Research, St. Charles, MO) and presented as mean \pm S.E.M. in $\mu\text{g/l}$.

Intraperitoneal Glucose Tolerance Test (IPGTT) *SSTR1/5^{-/-}* mice at days 7 and 150 after initial delivery of shRNA^{mousePDX-1} were fasted overnight before collection of blood samples as T0. Grouped mice were then given 1.2g glucose/kg body weight via ip injection followed by collection of blood samples at 15, 30, 60, and 120 min after injection of glucose. Glucose and insulin levels were measured as described above.

Necropsy, tissue collection, immunohistochemistry and TUNEL assay

Pancreatic and tumor tissue samples were obtained on days 0, 7, 21, 35, and end time after initial gene delivery. IHC was performed as described previously. Anti- PDX-1, insulin, PP, cyclin E, p27, Cdk4 or PCNA antibodies was applied to slides with 1:100 dilution followed by overnight incubation at 4°C. Slides were incubated with Cy3 or FITC-conjugated anti-rabbit, goat, or mouse secondary antibody depending on derivation of primary antibodies for one hour, and mounted with cover slides. TUNEL assay (FragELTM DNA Fragmentation Detection Kit, Colorimetric-TdT Enzyme, CALBIOCHEM, La Jolla, CA) was performed according to the manufacturer's protocol. The rate of apoptosis was expressed as the ratio of apoptotic cancer cells to the total number of endothelial cells in 10 fields at $\times 100$ magnification.

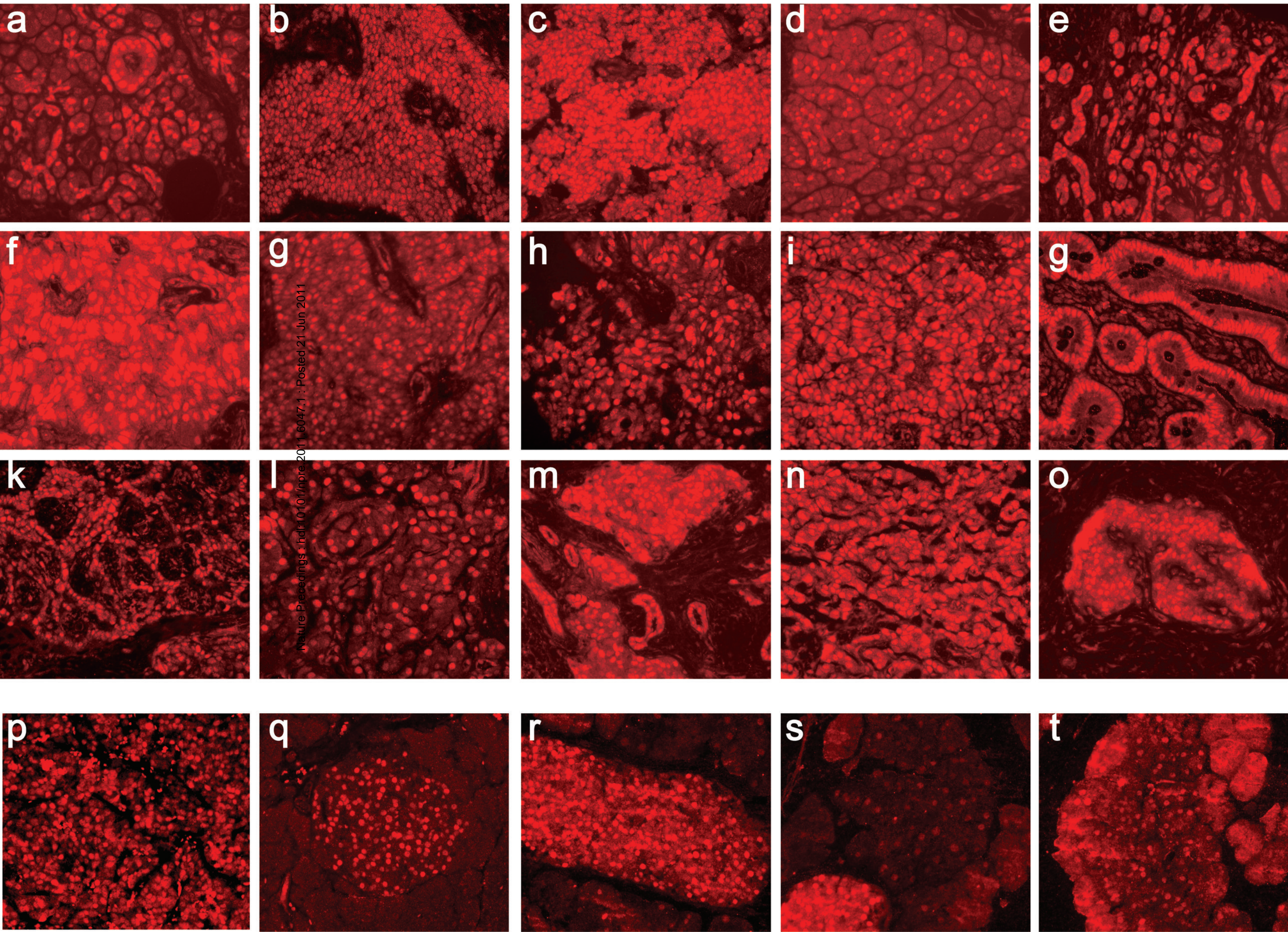
Statistical Analysis. The unpaired Student's *t*-test was used for statistical analyses of glucose levels, insulin levels, and cell proliferation with $P < 0.05$ indicating significance. The χ^2 test was used for rate comparison. Rank-log was used for mice survival comparison. Kaplan-Meier in SPSS 15.0 for MS Windows was used to plot survival curves.

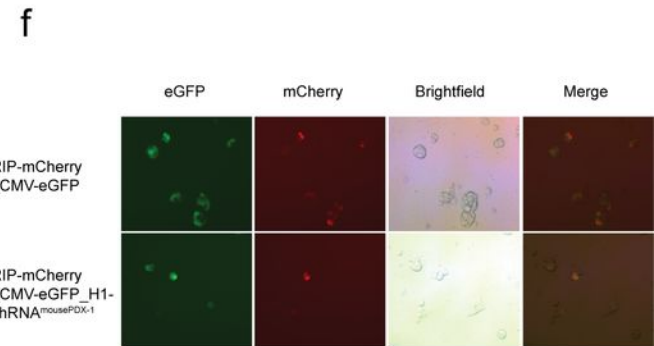
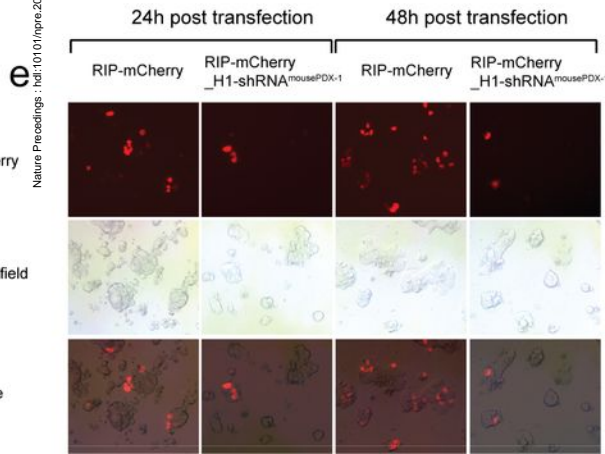
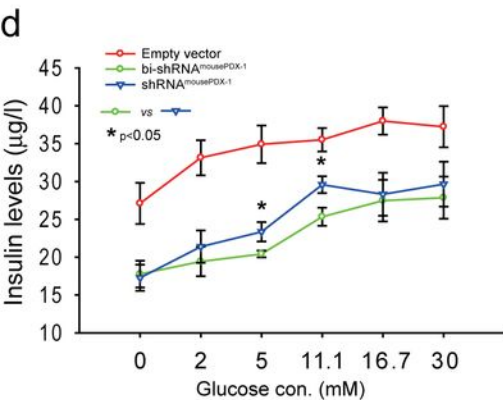
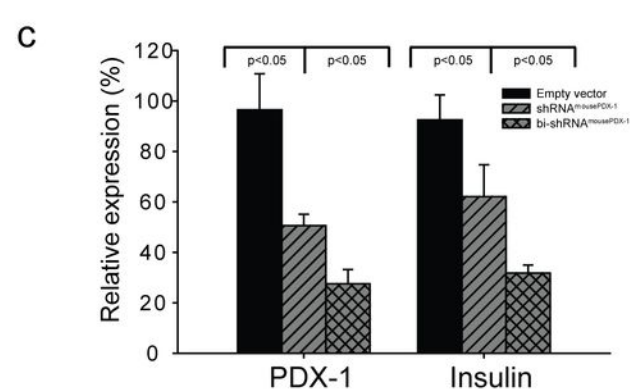
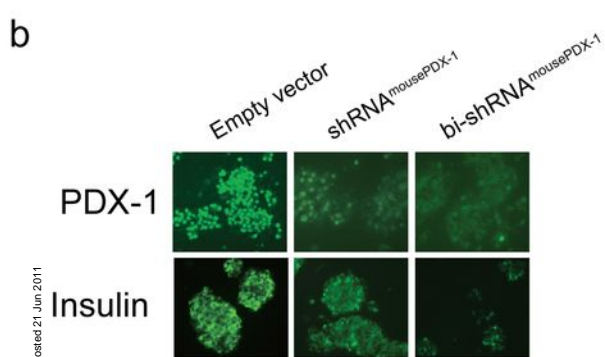
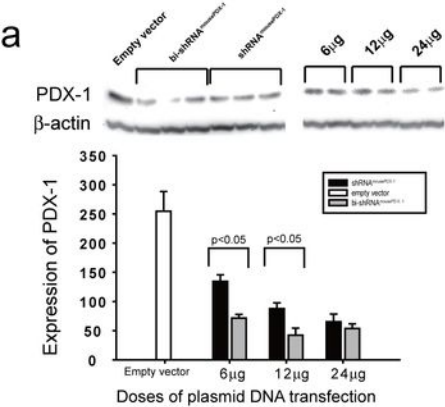
1. Offield, M.F., *et al.* PDX-1 is required for pancreatic outgrowth and differentiation of the rostral duodenum. *Development* **122**, 983-995 (1996).

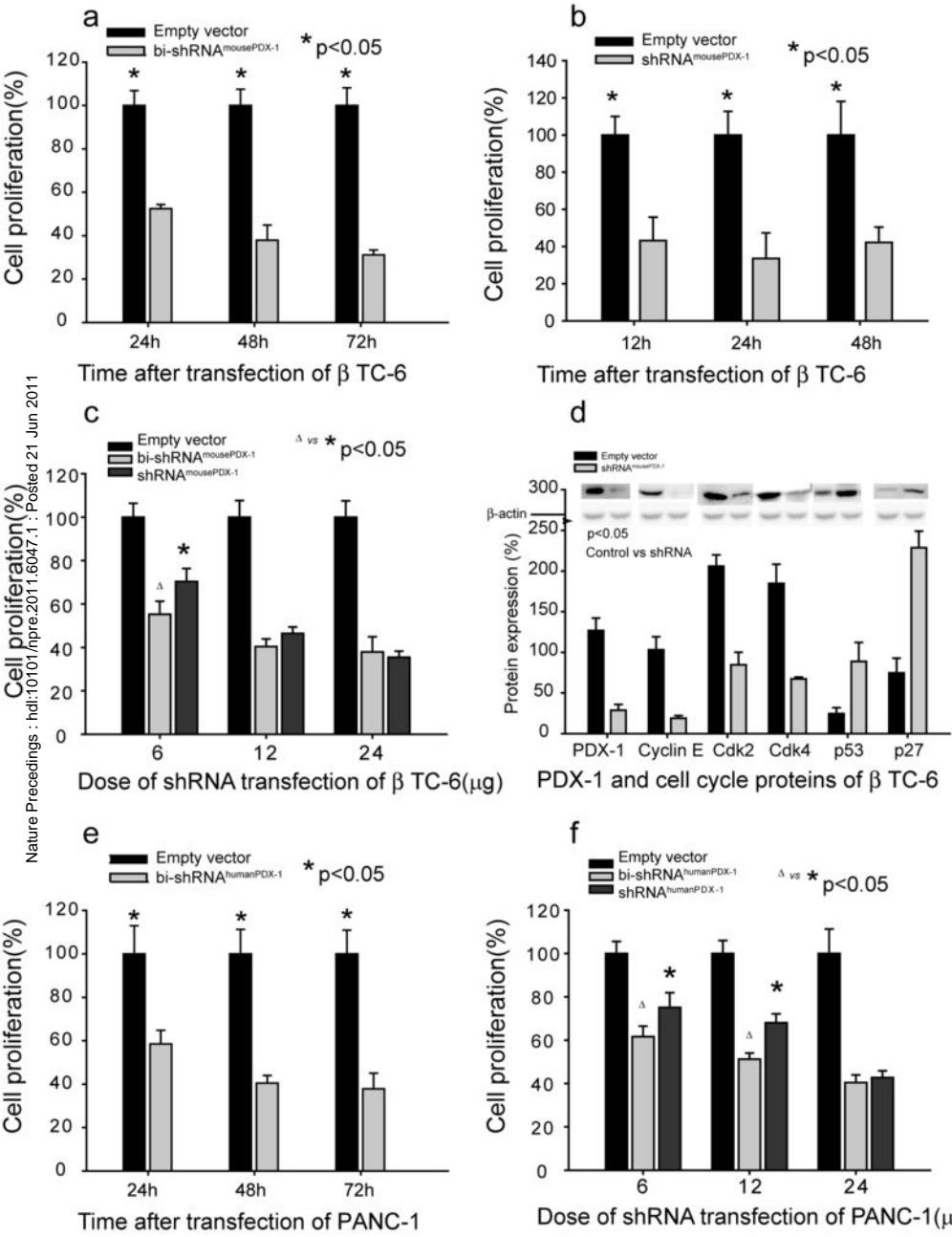
2. Hui, H. & Perfetti, R. Pancreas duodenum homeobox-1 regulates pancreas development during embryogenesis and islet cell function in adulthood. *Eur J Endocrinol* **146**, 129-141 (2002).
3. McKinnon, C.M. & Docherty, K. Pancreatic duodenal homeobox-1, PDX-1, a major regulator of beta cell identity and function. *Diabetologia* **44**, 1203-1214 (2001).
4. Gannon, M., *et al.* pdx-1 function is specifically required in embryonic beta cells to generate appropriate numbers of endocrine cell types and maintain glucose homeostasis. *Dev Biol* **314**, 406-417 (2008).
5. Iype, T., *et al.* Mechanism of insulin gene regulation by the pancreatic transcription factor Pdx-1: application of pre-mRNA analysis and chromatin immunoprecipitation to assess formation of functional transcriptional complexes. *J Biol Chem* **280**, 16798-16807 (2005).
6. Ashizawa, S., Brunnicardi, F.C. & Wang, X.P. PDX-1 and the pancreas. *Pancreas* **28**, 109-120 (2004).
7. Wolf, G., *et al.* The activation of the rat insulin gene II by BETA2 and PDX-1 in rat insulinoma cells is repressed by Pax6. *Mol Endocrinol* **24**, 2331-2342.
8. Wang, X.P., Li, Z.J., Magnusson, J. & Brunnicardi, F.C. Tissue MicroArray analyses of pancreatic duodenal homeobox-1 in human cancers. *World J Surg* **29**, 334-338 (2005).
9. Tirone, T.A., Fagan, S.P., Templeton, N.S., Wang, X. & Brunnicardi, F.C. Insulinoma-induced hypoglycemic death in mice is prevented with beta cell-specific gene therapy. *Ann Surg* **233**, 603-611 (2001).
10. Koizumi, M., *et al.* Increased PDX-1 expression is associated with outcome in patients with pancreatic cancer. *Surgery* **134**, 260-266 (2003).
11. Liu, S., *et al.* PDX-1 acts as a potential molecular target for treatment of human pancreatic cancer. *Pancreas* **37**, 210-220 (2008).
12. Stoffers, D., Ferrer, J., Clarke, W. & Habener, J. Early-onset type-II diabetes mellitus (MODY4) linked to IPF1. *Nature Genet* **17**, 138-139 (1997).
13. Shih, D.Q. & Stoffel, M. Molecular etiologies of MODY and other early-onset forms of diabetes. *Curr Diab Rep* **2**, 125-134 (2002).
14. Miyatsuka, T., *et al.* Persistent expression of PDX-1 in the pancreas causes acinar-to-ductal metaplasia through Stat3 activation. *Genes Dev* **20**, 1435-1440 (2006).
15. Li, Y., *et al.* Generation of insulin-producing cells from PDX-1 gene-modified human mesenchymal stem cells. *J Cell Physiol* **211**, 36-44 (2007).
16. Koizumi, M., *et al.* Pancreatic epithelial cells can be converted into insulin-producing cells by GLP-1 in conjunction with virus-mediated gene transfer of pdx-1. *Surgery* **138**, 125-133 (2005).
17. Wang, X., Zhou, J., Doyle, M.E. & Egan, J.M. Glucagon-like peptide-1 causes pancreatic duodenal homeobox-1 protein translocation from the cytoplasm to the nucleus of pancreatic beta-cells by a cyclic adenosine monophosphate/protein kinase A-dependent mechanism. *Endocrinology* **142**, 1820-1827 (2001).

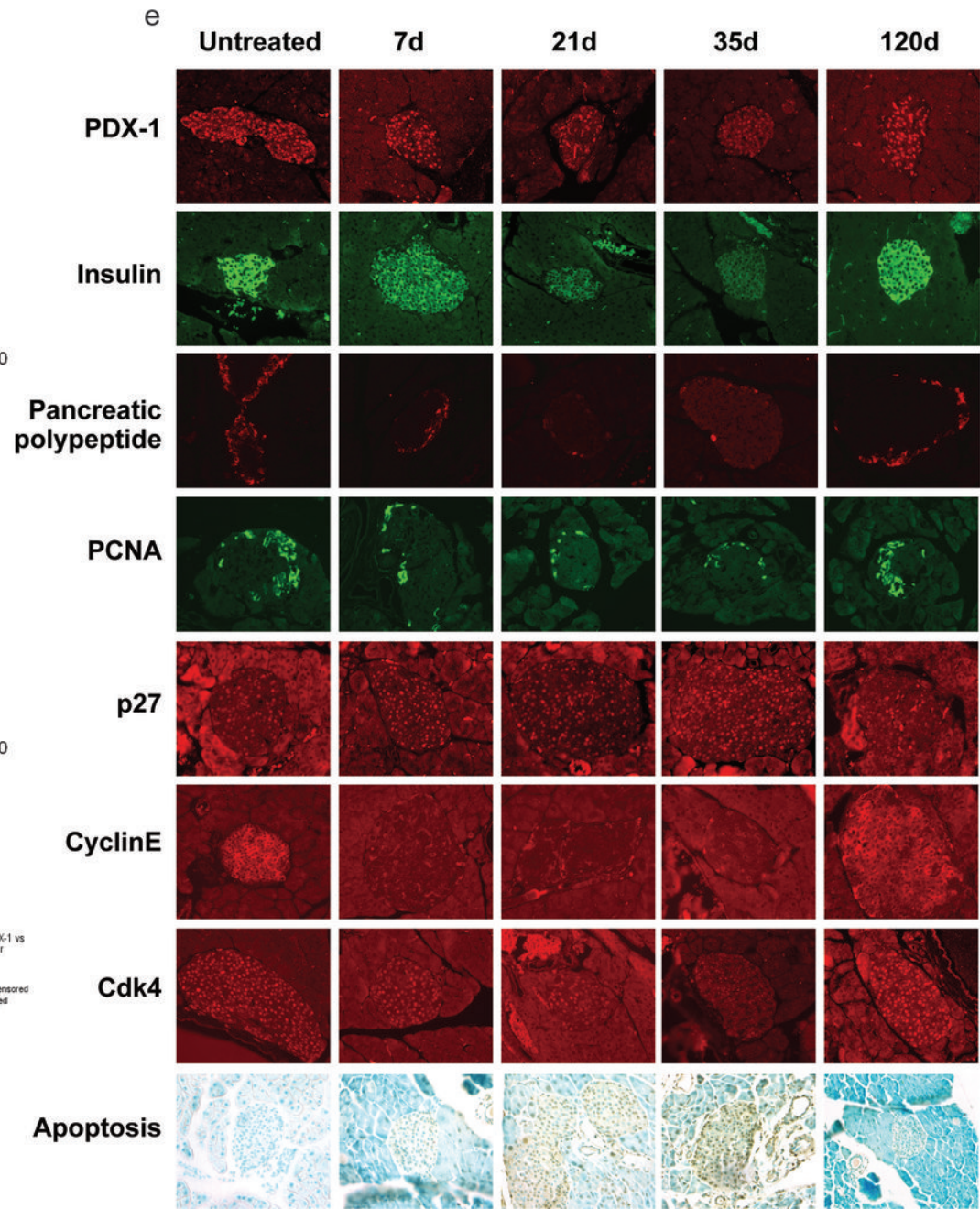
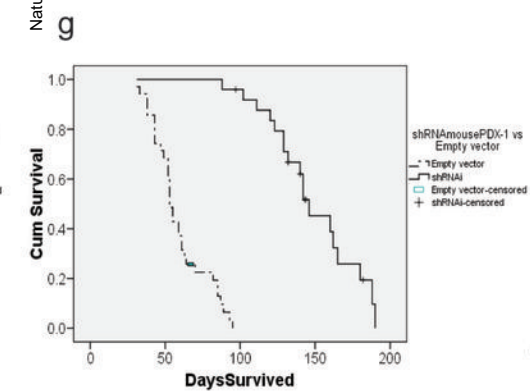
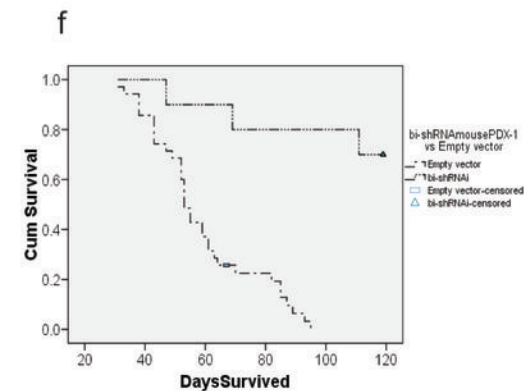
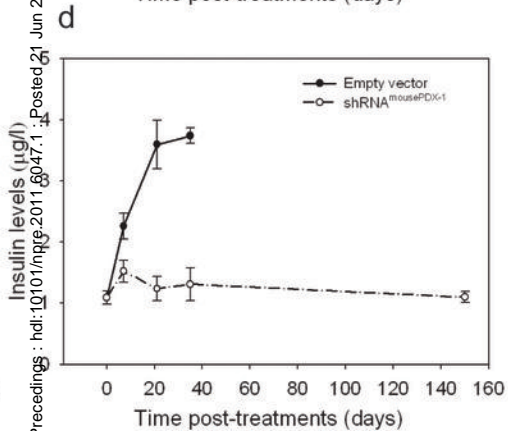
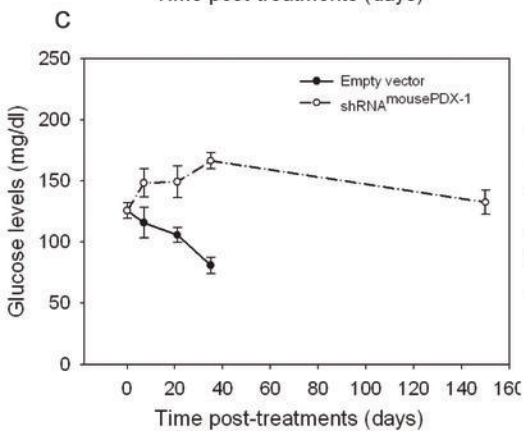
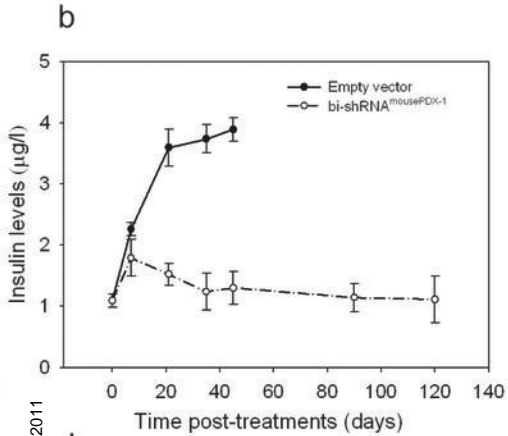
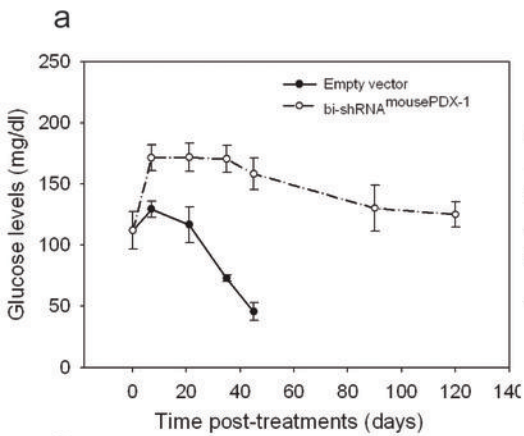
18. Aviv, V., *et al.* Exendin-4 promotes liver cell proliferation and enhances the PDX-1-induced liver to pancreas transdifferentiation process. *J Biol Chem* **284**, 33509-33520 (2009).
19. Zhou, J., Pineyro, M.A., Wang, X., Doyle, M.E. & Egan, J.M. Exendin-4 differentiation of a human pancreatic duct cell line into endocrine cells: involvement of PDX-1 and HNF3beta transcription factors. *J Cell Physiol* **192**, 304-314 (2002).
20. Zalzman, M., Anker-Kitai, L. & Efrat, S. Differentiation of human liver-derived, insulin-producing cells toward the beta-cell phenotype. *Diabetes* **54**, 2568-2575 (2005).
21. Watada, H., *et al.* PDX-1 induces insulin and glucokinase gene expressions in alphaTC1 clone 6 cells in the presence of betacellulin. *Diabetes* **45**, 1826-1831 (1996).
22. Carty, M.D., Lillquist, J.S., Peshavaria, M., Stein, R. & Soeller, W.C. Identification of cis- and trans-active factors regulating human islet amyloid polypeptide gene expression in pancreatic beta-cells. *J Biol Chem* **272**, 11986-11993 (1997).
23. Watada, H., *et al.* Involvement of the homeodomain-containing transcription factor PDX-1 in islet amyloid polypeptide gene transcription. *Biochem Biophys Res Commun* **229**, 746-751 (1996).
24. Serup, P., *et al.* Induction of insulin and islet amyloid polypeptide production in pancreatic islet glucagonoma cells by insulin promoter factor 1. *Proc Natl Acad Sci U S A* **93**, 9015-9020 (1996).
25. Bischof, L.J., *et al.* Characterization of the mouse islet-specific glucose-6-phosphatase catalytic subunit-related protein gene promoter by in situ footprinting: correlation with fusion gene expression in the islet-derived betaTC-3 and hamster insulinoma tumor cell lines. *Diabetes* **50**, 502-514 (2001).
26. Waeber, G., Thompson, N., Nicod, P. & Bonny, C. Transcriptional activation of the GLUT2 gene by the IPF-1/STF-1/IDX-1 homeobox factor. *Mol Endocrinol* **10**, 1327-1334 (1996).
27. Jepeal, L.I., *et al.* Cell-specific expression of glucose-dependent-insulinotropic polypeptide is regulated by the transcription factor PDX-1. *Endocrinology* **146**, 383-391 (2005).
28. Elbein, S., *et al.* Role of calpain-10 gene variants in familial type 2 diabetes in Caucasians. *J Clin Endocrinol Metab* **87**, 650-654 (2002).
29. Liu, S.H., *et al.* PDX-1: demonstration of oncogenic properties in pancreatic cancer. *Cancer* **117**, 723-733.
30. Liu, T., *et al.* Pancreas duodenal homeobox-1 expression and significance in pancreatic cancer. *World J Gastroenterol* **13**, 2615-2618 (2007).
31. Rao, D.D., *et al.* Enhanced target gene knockdown by a bifunctional shRNA: a novel approach of RNA interference. *Cancer Gene Ther* **17**, 780-791.
32. Rao, D.D., Senzer, N., Cleary, M.A. & Nemunaitis, J. Comparative assessment of siRNA and shRNA off target effects: what is slowing clinical development. *Cancer Gene Ther* **16**, 807-809 (2009).

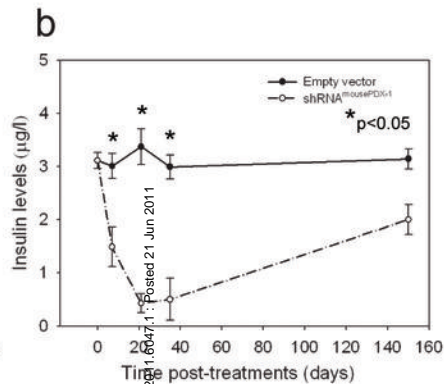
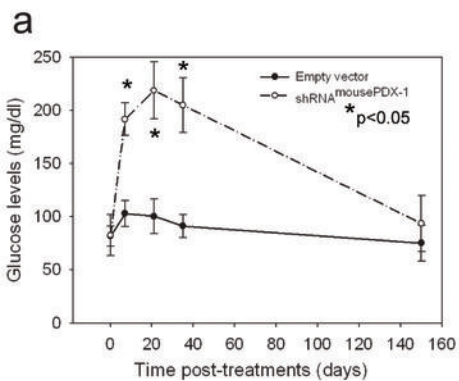
33. Rao, D.D., Vorhies, J.S., Senzer, N. & Nemunaitis, J. siRNA vs. shRNA: similarities and differences. *Adv Drug Deliv Rev* **61**, 746-759 (2009).
34. Templeton, N.S. Cationic liposome-mediated gene delivery in vivo. *Biosci Rep* **22**, 283-295 (2002).
35. Simberg, D., Weiss, A. & Barenholz, Y. Reversible mode of binding of serum proteins to DOTAP/cholesterol Lipoplexes: a possible explanation for intravenous lipofection efficiency. *Hum Gene Ther* **16**, 1087-1096 (2005).
36. Ramesh R, S.T., Templeton NS, Ji L, Stephens LC, Ito I, et al. Successful treatment of primary and disseminated human lung cancers by systemic delivery of tumor suppressor genes using an improved liposome vector. *Mol. Ther* **3**, 337-350 (2001).
37. Ito I, J.L., Tanaka F, Saito Y, Gopalan B, Branch CD, Xu K, Atkinson EN, Bekele BN, Stephens LC, Minna JD, Roth JA, Ramesh R Liposomal vector mediated delivery of the 3p FUS1 gene demonstrates potent antitumor activity against human lung cancer in vivo. *Cancer Gene Ther* **11**, 733-739 (2004).
38. Nemunaitis, G., et al. Hereditary inclusion body myopathy: single patient response to GNE gene Lipoplex therapy. *J Gene Med* **12**, 403-412 (2010).
39. Lu, C., et al. Systemic Gene Therapy with Tumor Suppressor FUS1-nanoparticles for Recurrent/Metastatic Lung Cancer. *J Clin Oncol* **28**, 15s (suppl.; abstract 7582) (2010).
40. Kaltsas, G.A., Besser, G.M. & Grossman, A.B. The diagnosis and medical management of advanced neuroendocrine tumors. *Endocr Rev* **25**, 458-511 (2004).
41. Wang, X.P., et al. The effect of global SSTR5 gene ablation on the endocrine pancreas and glucose regulation in aging mice. *J Surg Res* **129**, 64-72 (2005).
42. Wang, X.P., et al. Alterations in glucose homeostasis in SSTR1 gene-ablated mice. *Mol Cell Endocrinol* **247**, 82-90 (2006).
43. Wang, X.P., et al. Double-gene ablation of SSTR1 and SSTR5 results in hyperinsulinemia and improved glucose tolerance in mice. *Surgery* **136**, 585-592 (2004).
44. Wang, X.P., et al. SSTR5 ablation in islet results in alterations in glucose homeostasis in mice. *FEBS Lett* **579**, 3107-3114 (2005).
45. Moldovan, S., DeMayo, F. & Brunnicardi, F.C. Cloning of the mouse SSTR5 gene. *J Surg Res* **76**, 57-60 (1998).
46. Feanny, M.A., et al. PDX-1 expression is associated with islet proliferation in vitro and in vivo. *J Surg Res* **144**, 8-16 (2008).
47. Liu, T., et al. PDX-1 expression in pancreatic ductal cells after partial pancreatectomy in adult rats. *J Huazhong Univ Sci Technolog Med Sci* **24**, 464-466 (2004).
48. Taguchi, M., Yamaguchi, T. & Otsuki, M. Induction of PDX-1-positive cells in the main duct during regeneration after acute necrotizing pancreatitis in rats. *J Pathol* **197**, 638-646 (2002).



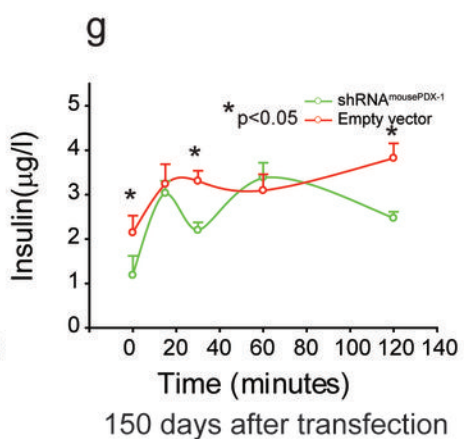
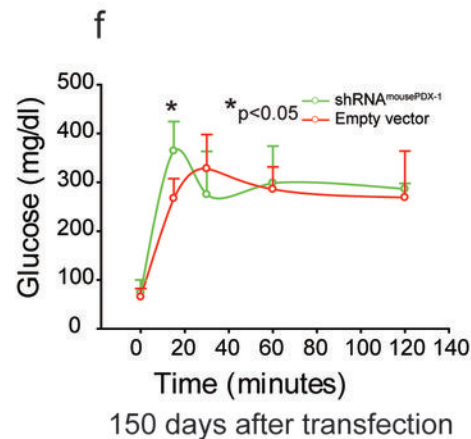
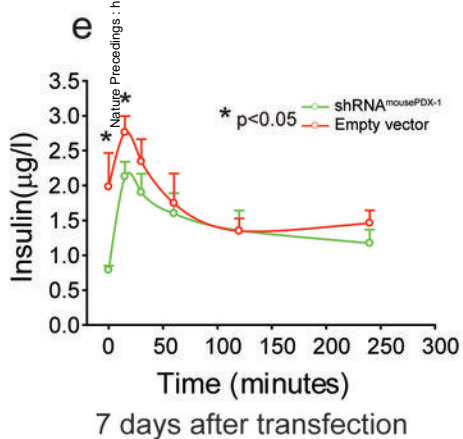
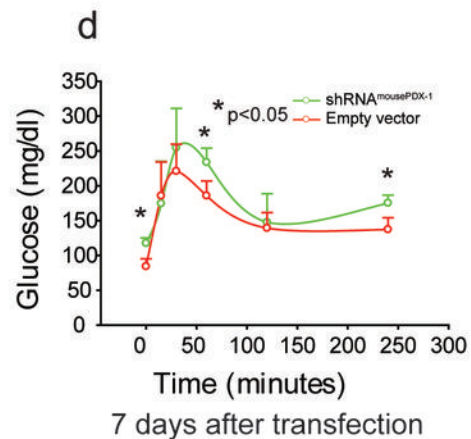
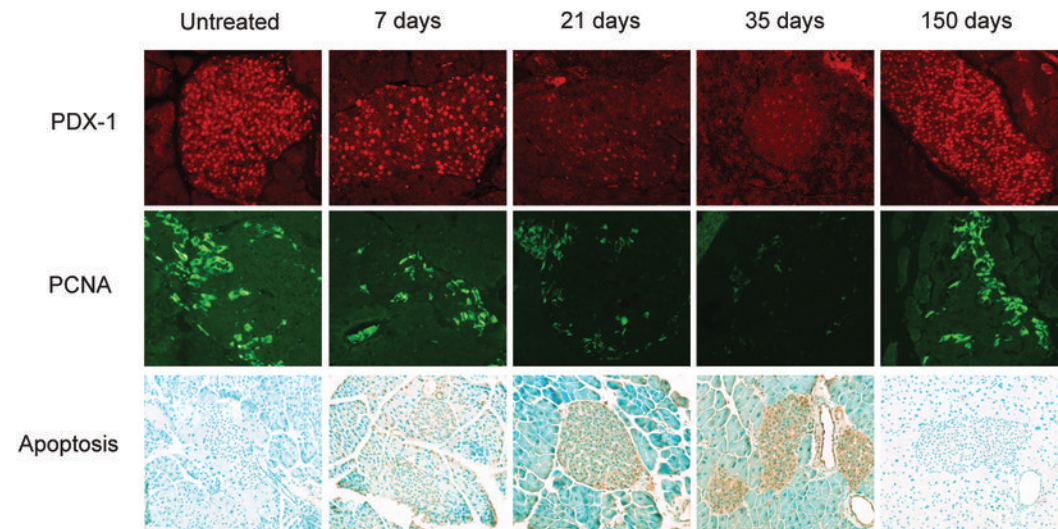


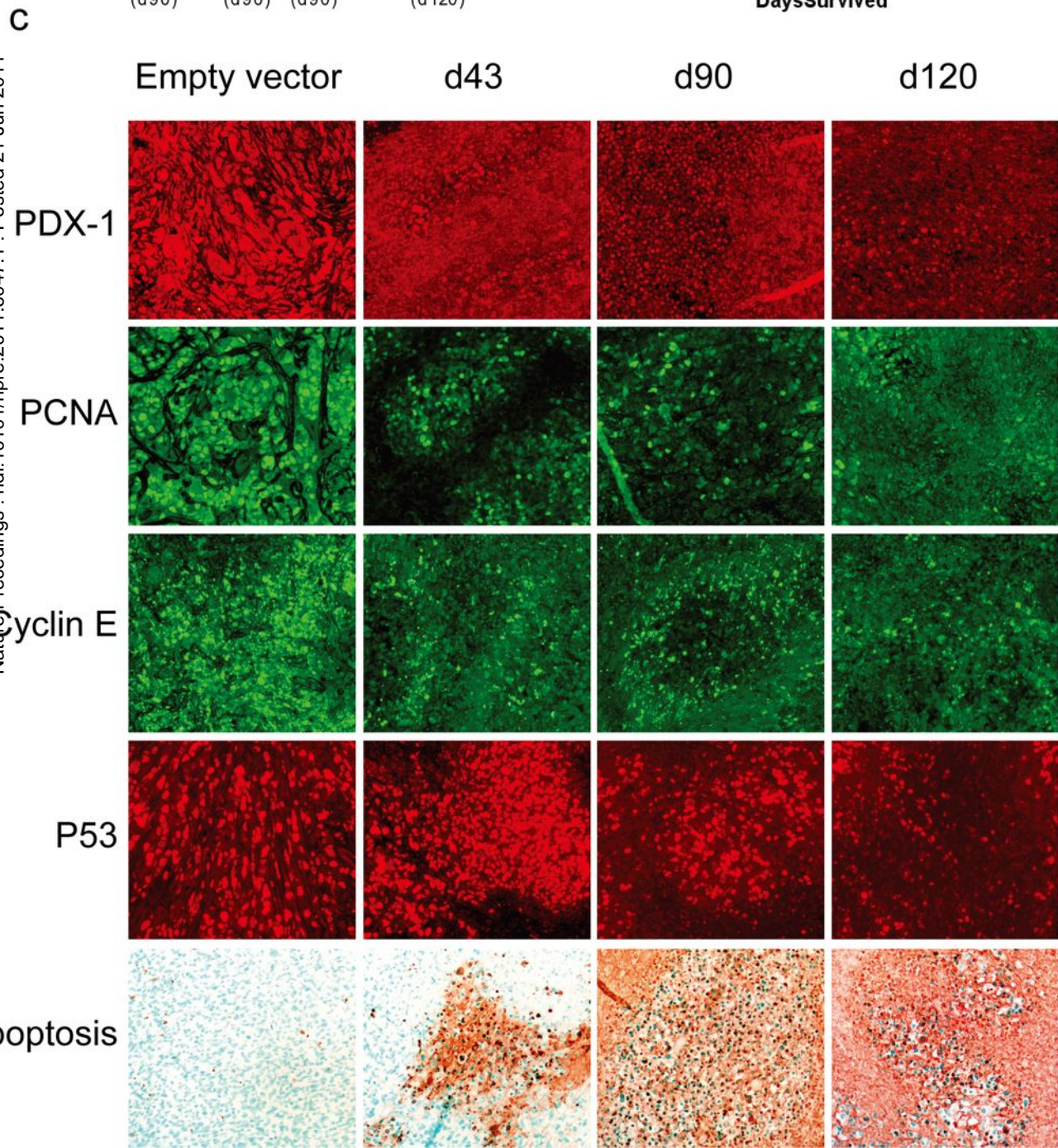
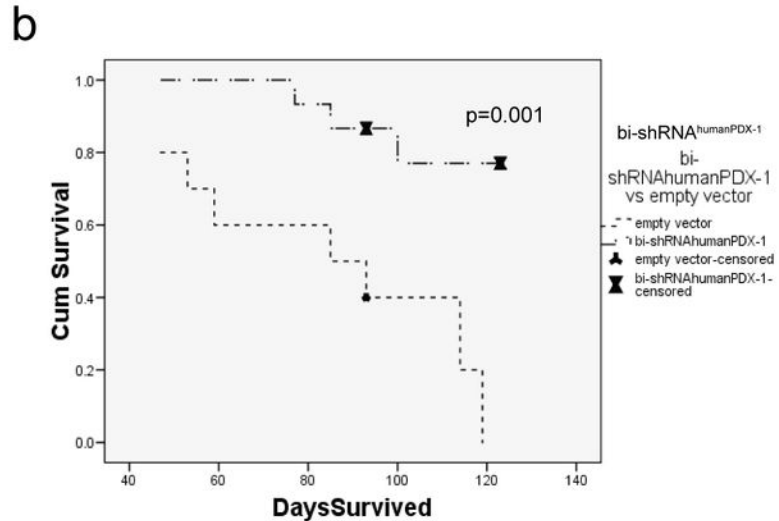
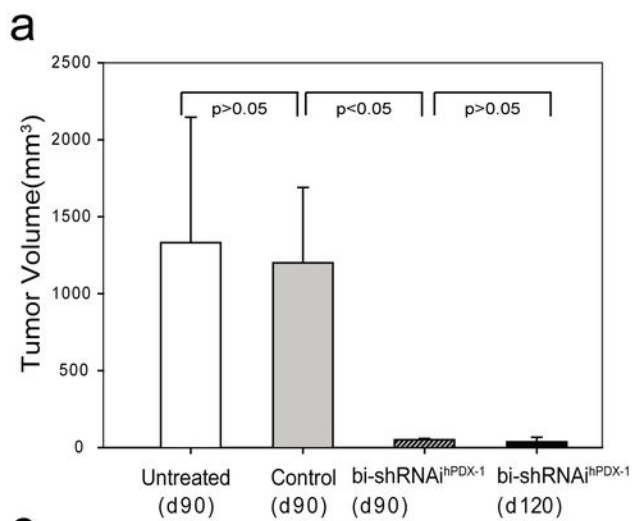


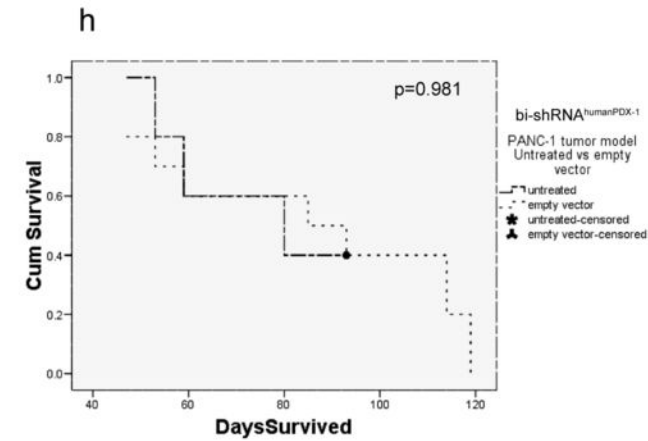
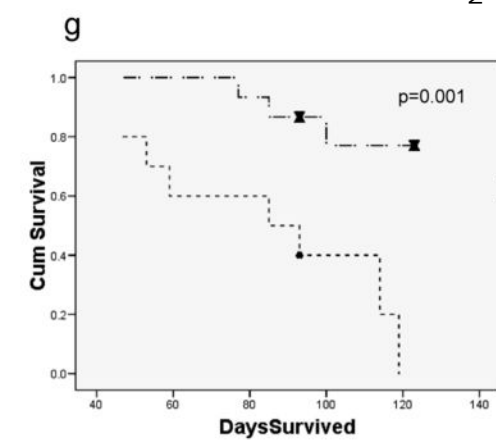
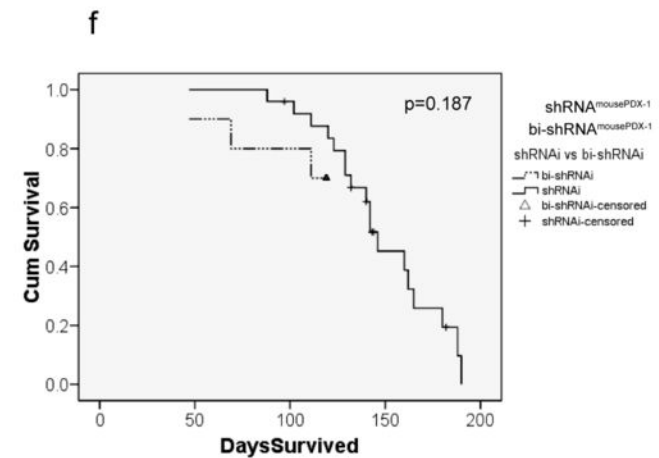
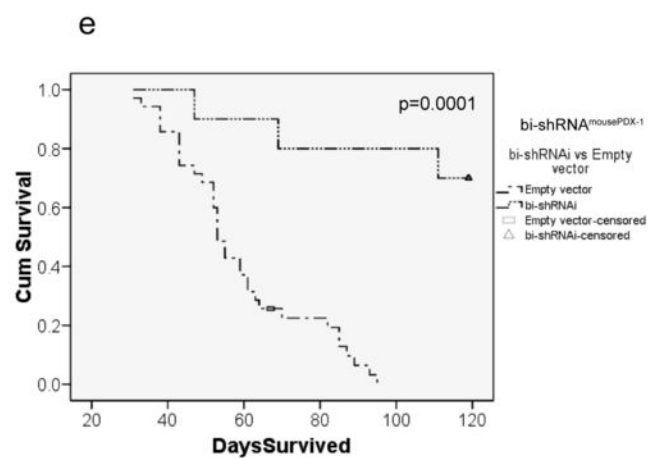
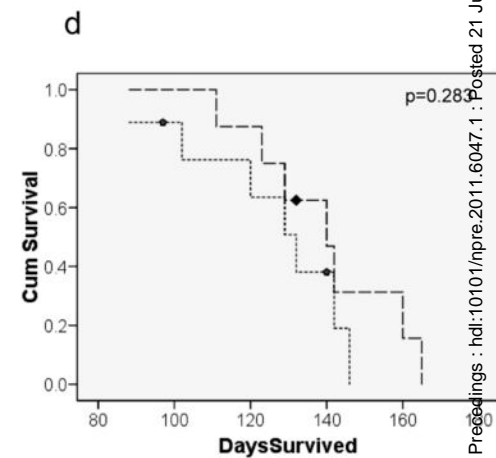
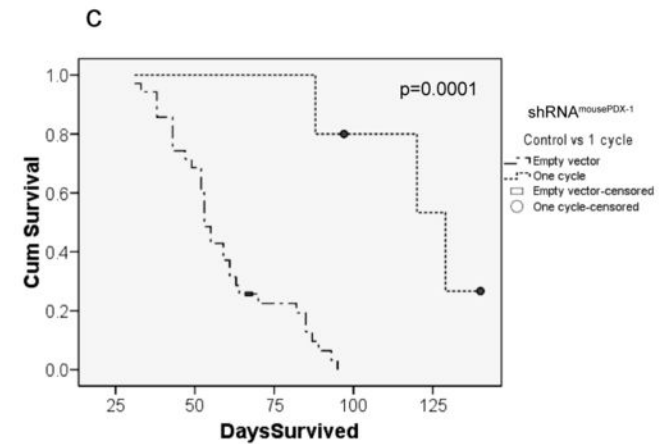
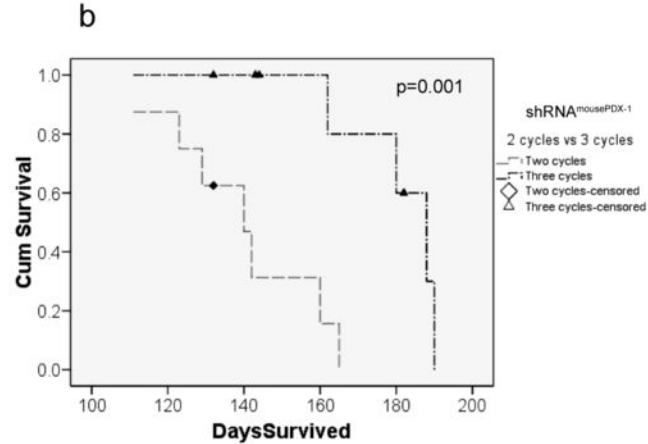
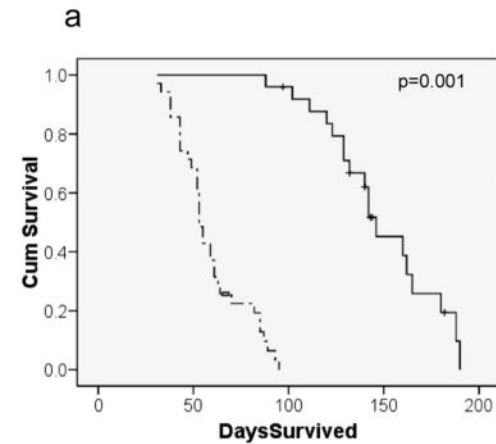




c



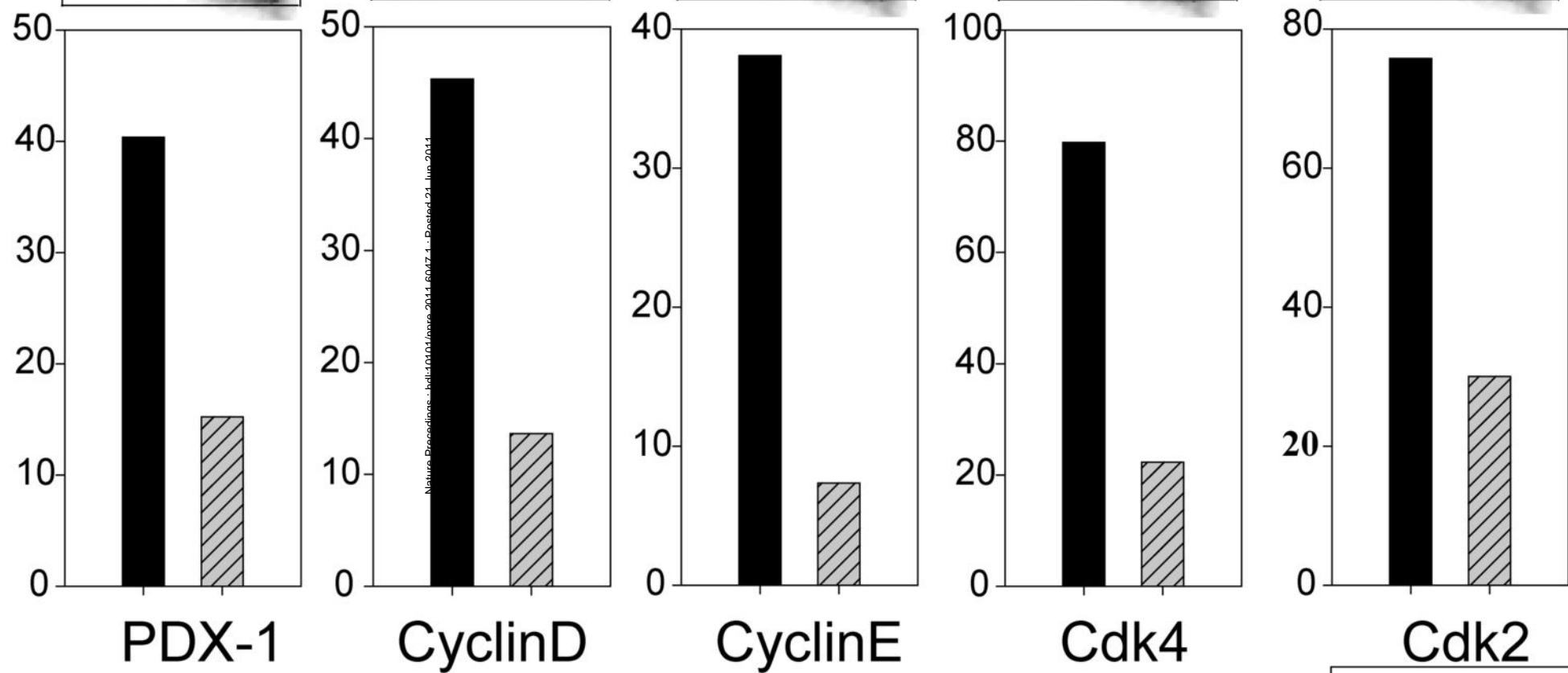




Nature Precedings : hdl:10101/npre.2011.6047.1 : Posted 21 Jun 2011

β -actin

Relative protein levels (%)



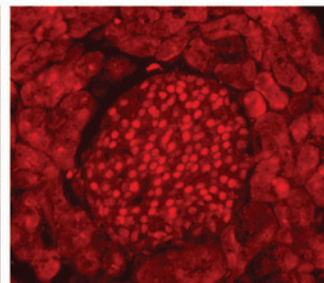
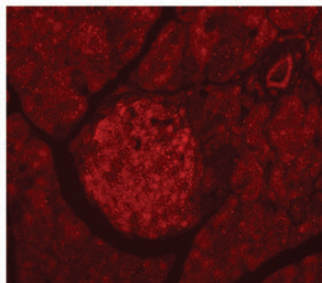
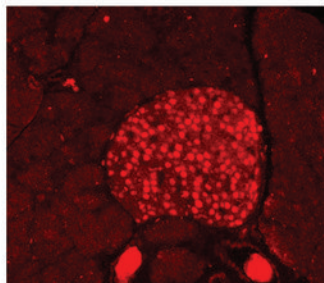
Vector control
shRNA^{mousePDX-1}

d0

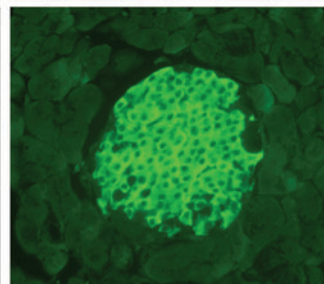
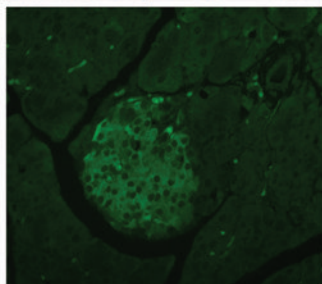
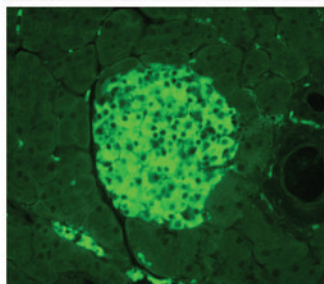
d43

d90

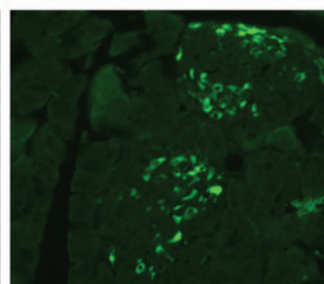
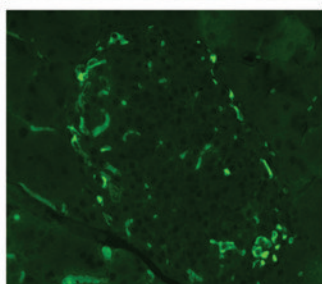
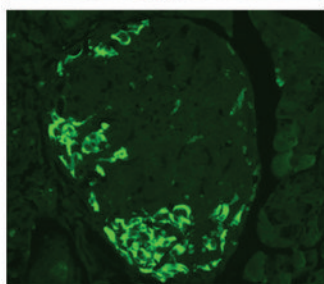
PDX-1



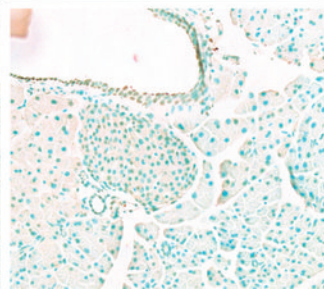
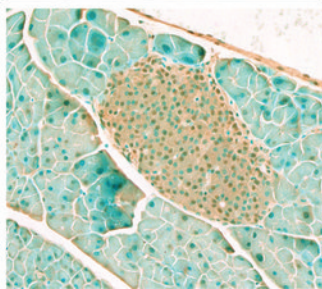
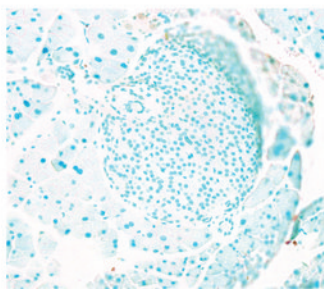
Insulin

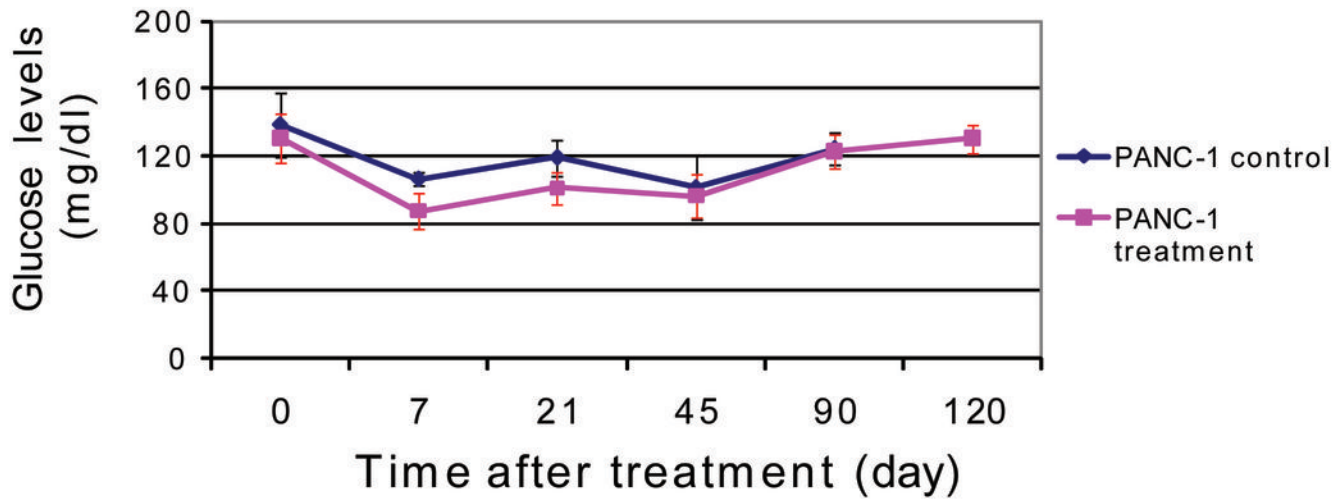
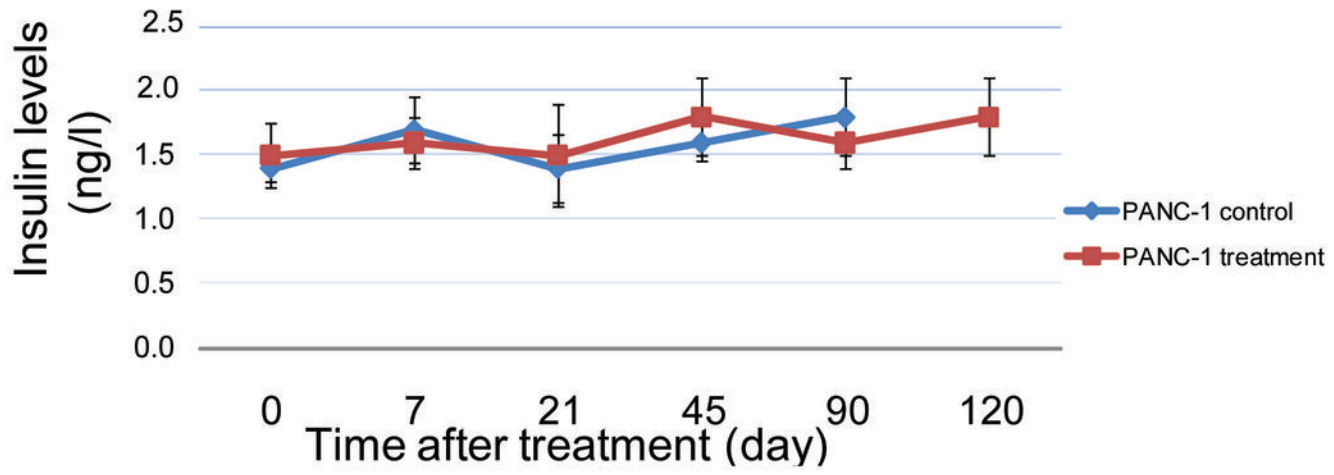


Pancreatic
Polypeptide



Apoptosis

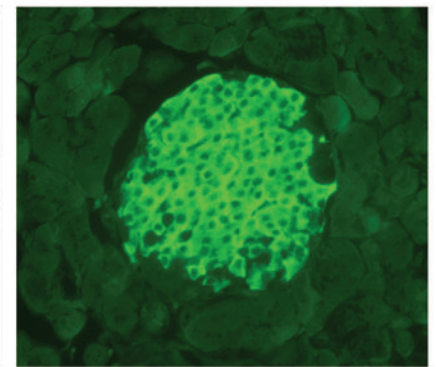
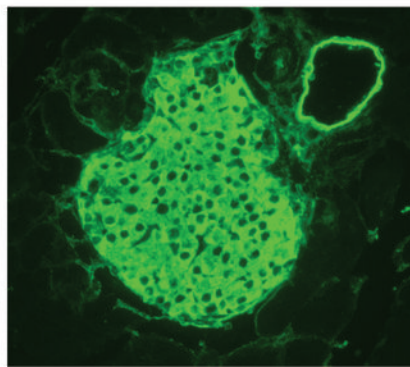
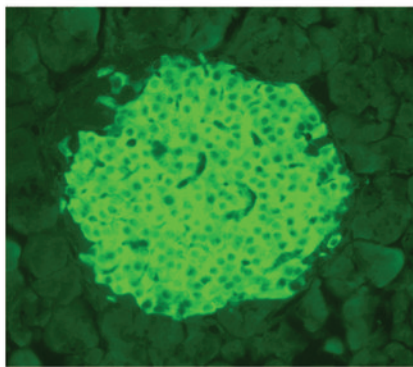
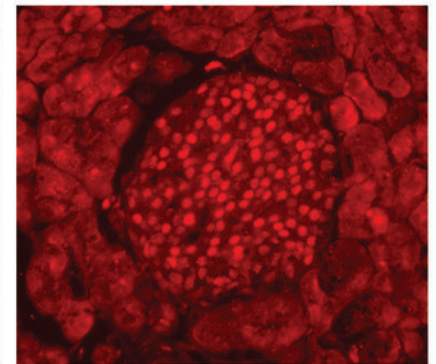
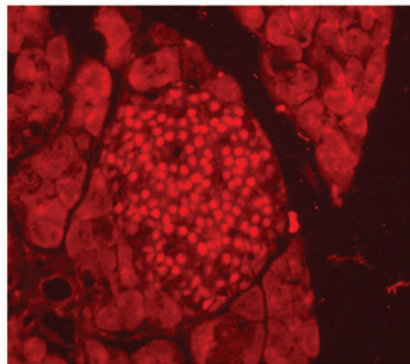
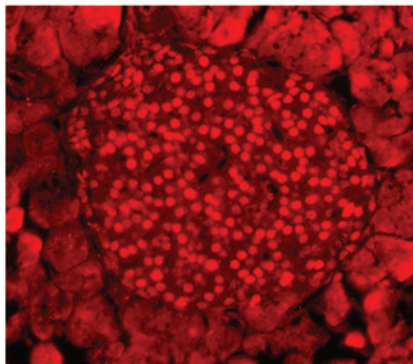




d0

d43

d120



PDX-1

Insulin